

Modeling coastal circulation in Norway using a high-resolution 4D-Var ocean assimilation system

Ann Kristin Sperrevik



Thesis for the degree of philosophiae doctor (PhD)
at the University of Bergen

2017

Date of defence: June 23, 2017

Abstract

The circulation along the Norwegian coast is characterized by many transient small-scale features such as eddies and meanders that are challenging to reproduce by means of numerical modeling. In this thesis I investigate the use of advanced data assimilation (DA) techniques in high-resolution coastal models to improve the circulation estimates.

One particularly interesting observational platform for the coastal ocean is high-frequency (HF) radars, which measure surface currents in the coastal zone up to 200 km offshore. The suitability of such observations for use in high-resolution coastal DA systems is assessed by quantifying which components of the near-surface current field are observed by the HF radars. Our results show that there are no contributions from wave drift in the measurements, thus they are suitable for use in coastal DA. Assimilation of HF radar currents in a high-resolution model shows clear improvement in the circulation estimates. Further improvement is obtained when CTD profiles of temperature and salinity are included in the assimilated data set.

A reanalysis of a period, during which in-situ observations were abundant in the study area, is used to assess how an observational network dense enough to constrain the water mass distribution affects the upper ocean circulation estimates. Our investigations of the results show a weakening of the topographically steered currents and, as the stratification increases the effective resolution of the model, more small-scale circulation features are developed. Such changes may have a significant effect on upper ocean transport. Finally, the potential of using high-resolution coastal reanalyses to study specific physical processes is demonstrated for the case of the mechanisms causing variability in the Norwegian Coastal Current.

List of papers

1. Röhrs, J., A. K. Sperrevik, K. H. Christensen, G. Broström, and Ø. Breivik: *Comparison of HF radar measurements with Eulerian and Lagrangian surface currents*, Ocean Dynamics **65**, 679-690, 2015.
2. Sperrevik, A. K., K. H. Christensen, and J. Röhrs: *Constraining energetic slope currents through assimilation of high-frequency radar observations*, Ocean Science **11**, 237-249, 2015.
3. Sperrevik, A. K., J. Röhrs, and K. H. Christensen: *Impact of data assimilation on Eulerian versus Lagrangian estimates of upper ocean circulation*, under revision for Journal of Geophysical Research - Oceans
4. Christensen, K. H. , A. K. Sperrevik, and G. Brostöm: *On the variability in the onset of the Norwegian Coastal Current*, Manuscript

Scientific environment

This PhD study has been carried out at the Norwegian Meteorological Institute, Division of Ocean and Ice, Oslo, Norway. A total of 4 weeks was spent at the University of California, Santa Cruz. The work has largely been funded by MET Norway, with contributions from the Norwegian Clean Seas Foundation (NOFO) and ENI Norge A/S, and the Norwegian Research Council through grants 244262 (RETROSPECT) and 237906 (CIRFA). Additional travel grants have been provided by ResClim.



**Norwegian
Meteorological
Institute**

Acknowledgements

First and foremost, I would like express my gratitude to my supervisor Kai H. Christensen. Your encouragement and support has been essential for the completion of this thesis, and I have truly learned a lot from you. I would also like to thank my co-supervisors Johnny A. Johannessen and Nils Gustafsson for sharing their insights and asking critical questions. A big thank you goes to Øyvind Breivik for his excellent guidance during the first year of the project, and to Øyvind Sætra who initiated this project.

I feel privileged to have been given the opportunity to conduct the research for my PhD project in the *Ocean and Ice* division at MET Norway and would like to thank all my colleagues for valuable discussions, advises and help. Johannes Röhrs deserves additional attention, as his contributions have lifted the quality of my research. Discussions with Frode Vikebø and Svein Sundby at the IMR have expanded my horizon, thank you! Thanks also to Andy Moore for welcoming me at University of California, Santa Cruz and for taking an interest in my research.

To my family and friends: thanks for your continued support and encouragement. Finally, a huge thank you to my ever-patient husband Tormod, who has provided both technical as well as emotional support.

Contents

Abstract	i
List of papers	iii
Scientific environment	v
Acknowledgements	vii
1 Introduction and Objectives	1
1.1 Introduction	1
1.2 Objectives	2
2 Scientific background	5
2.1 The Norwegian Shelf Seas	5
2.2 Data Assimilation	6
2.3 Observations	10
3 Tools and Methods	13
3.1 ROMS	13
3.2 ROMS-4DVAR	13
4 Summary and future perspective	17
4.1 Summary of papers	17
4.2 Perspectives	19
5 Scientific papers	27
5.1 Comparison of HF radar measurements with Eulerian and Lagrangian surface currents	29
5.2 Constraining energetic slope currents through assimilation of high- frequency radar observations	43
5.3 Impact of data assimilation on Eulerian versus Lagrangian estimates of upper ocean circulation	59
5.4 On the variability in the onset of the Norwegian Coastal Current	77

Chapter 1

Introduction and Objectives

1.1 Introduction

Human activities at sea such as shipping, oil exploitation, fisheries, and recreation largely occur in the coastal ocean and shelf seas. These regions are also important for marine life as they serve as spawning and feeding grounds for several fish stocks, such as the Northeast Arctic cod, and are hot spots for primary production in the ocean. Circulation estimates from operational forecasts are key components of emergency response services such as search-and-rescue and oil spill mitigation (Breivik and Allen, 2008; Jordi et al., 2006; Röhrs and Christensen, 2015), while data archives of the ocean state during a historic period can be used e.g. for studies of physical processes, connectivity studies (Ådlandsvik and Sundby, 1994; Mitarai et al., 2009), or to assess the mechanisms causing inter-annual variability in recruitment (Svendsen et al., 2007). For many such purposes, the currents in the uppermost part of the ocean are most relevant.

Upper ocean currents are largely wind-driven, but particles drifting in the sea are also affected by transient current features such as tides and eddies as well as large-scale geostrophic currents. Eddies are the oceanic equivalent to high and low pressure systems in the atmosphere, but their horizontal scales are much smaller due to the shorter internal deformation radius in the ocean. In order to provide realistic estimates of ocean currents this scale needs to be resolved by the model. High resolution also allows for a more accurate description of the bathymetry and a more detailed coastline, an important point as many accidents happen close to shore (Broström et al., 2011; Gundlach and Hayes, 1978) and the environmental consequences of a spill often will be more pronounced in the coastal zone (Ihaksi et al., 2011).

A realistic representation of water masses is crucial for the skill of an ocean model, as this affects the baroclinic response to surface forcing, as well as the generation of eddies through baroclinic instabilities occurring at fronts between water masses of different densities. Furthermore, the depth at which a buoyant particle will flow is determined by the density of the surrounding water. As both the strength and direction of wind-driven currents are depth dependent, this will affect the particle's path (Hannah et al., 1997; Myksovoll et al., 2014; Vikebø et al., 2007).

In addition to the small spatial scales, the ocean has a long memory. This means that features such as eddies will persist over several days to weeks, and water properties, particularly below the mixed layer, for even longer periods of time. Due to these long temporal scales errors in ocean models can largely be viewed as caused by deficien-

cies in the initial conditions. For small regional applications, however, the boundary values become more important, particularly for the upper ocean where the currents are generally stronger. Similar to the case of limited area models in numerical weather prediction, errors due to unresolved physical processes in the coarser model from which the boundary conditions are provided, propagate into the model domain (Warner et al., 1997). Thus, coastal ocean modeling is both an initial and a boundary value problem, and in order to produce realistic estimates of the coastal circulation, errors in both these sources need to be constrained.

Data assimilation (DA) can improve a model estimate of the ocean state by adjusting the model fields according to observations. DA methods take both uncertainties associated with the model fields as well as uncertainties associated with the observations into account, thus DA combines an inaccurate model with inaccurate observations in order to obtain the best possible description, an analysis, of the true state of the ocean. However, the resolution of the model poses a limit to the precision of the analysis: Even if there are sufficient observations to describe an eddy, the model is incapable of reproducing it if the size of the eddy is too small to be resolved numerically. This is referred to as the error of representativeness, and is usually the largest source of uncertainty associated with an observation.

DA has been a large contributor to the improved quality of weather forecasts over the past few decades, and is commonly used in operational oceanography as well, especially for global and basin-scale applications (Blockley et al., 2014; Oke et al., 2015a; Sakov et al., 2012). In contrast to the observational network for the atmosphere, the oceanic observational network does not resolve the spatial variability, particularly below the surface. This is a major challenge for high-resolution assimilation systems as they require a denser observational network to constrain the circulation (Oke et al., 2015b). One particular challenge is the inherent lack of current observations: with the notable exception of high-frequency (HF) radars which can observe surface currents in the coastal zone, there are hardly any observations of this important variable.

1.2 Objectives

The main objective of this thesis is to study the requirements that must be met by the ocean model and the observing system in order to obtain improvement in the representation of upper ocean circulation in high-resolution coastal ocean models. A second aim is to determine whether assimilation of existing and planned observational networks can improve circulation estimates of the coastal ocean. In a long-term perspective we hope to develop methodology for improving operational ocean forecasts and for giving recommendations on the design of future observational networks supporting this aim. Specifically, the following points are targeted:

- Assessing the potential impact on forecast skill when assimilating HF radar observations of surface currents.
- Understanding how assimilation of hydrography observations impact near-surface circulation estimates.
- Investigate if information from different observation types complement each other or render some observations redundant.

- Use a reanalysis of the ocean state in coastal region to investigate the mechanisms causing variability in the circulation, and to what degree the different observation sources contribute to the improved circulation estimates.

To answer these questions, coastal model applications using four-dimensional variational (4D-Var) assimilation techniques have been applied, assimilating various types of ocean observations. The main focus of the investigations of the results is the impact on the upper ocean circulation, an important component in ocean forecasting.

Chapter 2

Scientific background

2.1 The Norwegian Shelf Seas

The Norwegian coastline is long and complex, scattered with numerous islands and skerries. Fjords add to the complexity: some stretch more than 100 km inland, and many fjords are deeper than the adjacent seas. Norway borders four marginal seas. Starting from the north these are the shallow Barents Sea; the Norwegian Sea, which has a shallow shelf along the Norwegian coast with a steep shelf break into the deep basin; the North Sea, another shallow shelf sea; and Skagerrak in the south. Skagerrak is shallow apart from the Norwegian Trench, an underwater canyon stretching from the shelf break outside western Norway and along the coast into Skagerrak where it reaches its maximum depth of 700 m (Fig. 2.1).

Skagerrak serves as the only natural connection of the Baltic Sea with adjacent seas, and the circulation is heavily influenced by the freshwater outflow from the Baltic. This outflow gives rise to the Norwegian Coastal Current (NCC), which carries fresh coastal water northwards along the coast. Although additional freshwater is supplied from rivers and fjords along the coast, the water of the NCC becomes more saline as it moves northwards due to entrainment of waters of Atlantic origin. Atlantic water, defined as water with salinity above 35, enters the Norwegian Sea through three passages: The Denmark Strait, the opening between Iceland and the Faroe Islands, and through the Faeroe-Shetland channel. The water associated with the latter two inflows forms The Norwegian Atlantic Current (NAC), and flows northward along the eastern rim of the Norwegian Sea. Minor branches of the NAC break off from the main path and flows into the North Sea and along the Norwegian Trench into the Skagerrak. On its way northward, the NAC flows in near-parallel with the NCC before the two currents partly converge outside Vesterålen, where the continental shelf is at its narrowest. This region is highly dynamic with current speeds often exceeding 1 m/s and high eddy kinetic energy levels (Isachsen et al., 2012). As the currents continue northwards, the main branch of the NAC breaks off from the coast and follows the shelf break towards Spitsbergen and into the Arctic Ocean, while the NCC continues along the coast into the Barents Sea.

The NCC is often described as being wedge-shaped, and this shape has a strong seasonal dependence arising from both seasonal varying runoff levels and variations in the solar insolation. Increased freshwater supply and solar warming during the summer months result in a broad and shallow current wedge, while surface cooling and low

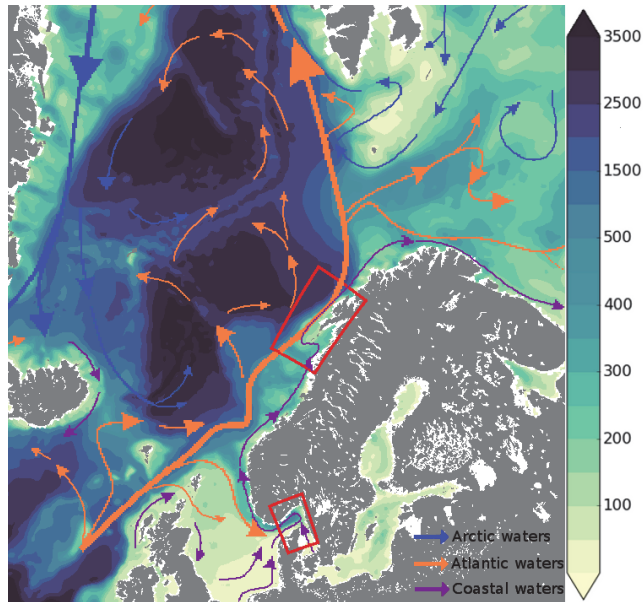


Figure 2.1: Map of Norwegian waters. The bathymetry is indicated in shading, while the arrows display the main currents. The two model domains used in the thesis papers are shown in red. The currents are reproduced from graphic by IMR (http://www.imr.no/nyhetsarkiv/2006/november/ingen_stopp_i_golfstrommen/nb-no).

runoff levels during the winter season makes the wedge deep and narrow (Saetre, 2007).

The tidal signal along the Norwegian Coast is dominated by a tidal wave entering the Norwegian waters from the North Atlantic and propagating northwards along the coast as a Kelvin wave (Saetre, 2007). The tidal amplitude varies significantly, with generally small amplitudes found in Skagerrak, amplitudes close to zero outside Egersund in southwestern Norway where an amphidromic point is found, and amplitudes close to 4 m in Northern Norway. The dominating tidal constituents are the diurnal lunar and solar components, M2 and S2.

Providing realistic estimates of the highly dynamic circulation of this coastal region poses a challenge for numerical models. In particular, the pronounced front separating the fresh water of the NCC from Atlantic waters has proven to be difficult to reproduce (e.g. Budgell, 2005; Lien et al., 2013; Røed and Albretsen, 2007; Winther and Evensen, 2006). In this thesis we apply high-resolution models constrained by observations that are assimilated into the model fields to produce circulation estimates.

2.2 Data Assimilation

The use of data assimilation (DA) to prepare high-quality initial conditions for numerical weather prediction (NWP) models is of key importance to ensure reliable weather forecasts. DA is also an essential tool for reconstructing the atmospheric or oceanic state during a past period in a consistent way. When DA is used in this way the re-

sulting data set is called a reanalysis. Such data sets provide long time series of high resolution that cannot be matched by observations alone, and are invaluable for the scientific community.

As DA in ocean models largely builds on development made within the field of NWP, the information presented in this section will be given in this context. This section leans on several texts on data assimilation, such as Blayo et al. (2014); Bouttier and Courtier (1999); Fisher (2010); Kalnay (2003); Talagrand (1997) .

The first approaches to adjust initial conditions for the purpose of weather forecasting include adjusting weather maps by hand according to the available observations, and for the first generation of numerical models, interpolation of the observations to the model grid. Prior to the satellite era, observations tended to be unevenly distributed in space, with many observations over populated areas and hardly any over uninhabited parts of the world. This motivated the development of methods which combined a background state from the numerical model itself with the available observations (Bergthorsson and Döös, 1955).

The development of modern DA techniques was motivated by two important advances in NWP. First, the famous discovery by Lorenz (1963) that even small perturbations (on the order of roundoff errors) in the initial condition of a dynamical system would yield different solutions. Second, the fact that primitive equation models, introduced in the early seventies, are more sensitive to their initial conditions than the first generation of numerical models. In order to obtain initial conditions that would limit the error growth and ensure a stable model run after assimilation, modern DA techniques aims to assimilate observations into the model fields in a way that not only brings the model closer to the true state, but is also consistent with the dynamics represented by the model. The latter point is important, as fast gravity-inertia wave oscillations may quickly deteriorate the model solution if the analysis state is not properly balanced.

All state-of-the-art assimilation methods build on a statistical approach, in which a background state (\mathbf{x}_b), observations (\mathbf{y}), and description of the error variances of both former terms are combined to provide the best possible description of the true state (\mathbf{x}_t), the so-called analysis (\mathbf{x}_a). “Best possible” is here defined as the state that minimizes the analysis error variance. The errors are defined as

$$\begin{aligned}\mathcal{E}_a &= \mathbf{x}_a - \mathbf{x}_t \\ \mathcal{E}_b &= \mathbf{x}_b - \mathbf{x}_t \\ \mathcal{E}_o &= \mathbf{y} - H(\mathbf{x}_t),\end{aligned}$$

where H is an observation operator that maps between model space and observation space. Assuming that the mean errors of both observations and background state are zero, and that there is no correlation between the errors of the two, the best linear unbiased estimate can be defined as

$$\mathbf{x}_a = \mathbf{x}_b + \mathbf{K}(\mathbf{y} - H(\mathbf{x}_b)), \quad (2.1)$$

where the model state variables, $\mathbf{x}_{a,b}$ consist of all prognostic model variables at every grid point, and \mathbf{K} is the gain matrix that determines the weighting of observations and background state. H may be a simple interpolation operator, or in addition contain a

function relating model variables to an observed quantity, e.g. radial current as measured by a HF radar. H is often assumed to be perfect, i.e. no errors are introduced in the mapping from model space to observation space. It is also often assumed that the observation operator (H) can be linearized, so that for a small increment $\delta\mathbf{x}$ to \mathbf{x} we have

$$H(\mathbf{x} + \delta\mathbf{x}) = H(\mathbf{x}) + \mathbf{H}(\delta\mathbf{x}). \quad (2.2)$$

When a solution to Eq. (2.1) is sought by finding the analysis that yields the smallest value for the analysis error variance, \mathbf{K} is the Kalman gain matrix

$$\mathbf{K} = \mathbf{B}\mathbf{H}^T(\mathbf{H}\mathbf{B}\mathbf{H}^T + \mathbf{R})^{-1}, \quad (2.3)$$

where \mathbf{R} and \mathbf{B} are the covariance matrices for the observation errors and the model background errors, respectively. As the full covariance matrix for the model background errors is usually not well known, and is too large to be used in practice, \mathbf{B} can only be approximated. For the case of uncorrelated errors, \mathbf{R} is easier to specify, and is commonly assumed to be known. It consists of two parts: the instrumental error describing the expected accuracy of the measurement, and the error of representativeness which relates to how well the observed quantity can be represented in the model. E.g., the current at a given location in the ocean may be measured with high precision, however, if this observation is to be assimilated into a model of finite resolution, the observed current may be a poor measure of the currents resolved by the model, and thus have a large representation error.

Currently, the methods for solving the DA problem within the context of NWP can be divided in two categories: ensemble methods, in which the ensemble spread is used to specify \mathbf{B} , and variational methods. The 4D-Var method applied in this thesis belongs to the latter category. Variational methods can be described by a maximum likelihood approach, as the idea is to find the most probable state given the available information provided by the observations and the background: $\mathbf{x}_a = \max p(\mathbf{x}|\mathbf{y} \wedge \mathbf{x}_b)$, where p is a probability density function. According to Bayes theorem, we have

$$p(\mathbf{x}|\mathbf{y} \wedge \mathbf{x}_b) = \frac{p(\mathbf{y} \wedge \mathbf{x}_b|\mathbf{x})p(\mathbf{x})}{p(\mathbf{y} \wedge \mathbf{x}_b)}, \quad (2.4)$$

in which the denominator is independent of \mathbf{x} , and since \mathbf{x} is unknown all choices of \mathbf{x} have equal probability, rendering $p(\mathbf{x})$ a constant. Thus, the left hand side of Eq. (2.4) is proportional to the remaining terms on the right. When applying the assumption of uncorrelated observation and background errors, we get the expression

$$p(\mathbf{x}|\mathbf{y} \wedge \mathbf{x}_b) \propto p(\mathbf{y}|\mathbf{x})p(\mathbf{x}_b|\mathbf{x}). \quad (2.5)$$

Eq. (2.5) may be expressed in the form of a cost function, and when simultaneously using the fact that the logarithm is a monotonic function, we get the following expression:

$$J(\mathbf{x}) = -\log(p(\mathbf{y}|\mathbf{x})) - \log(p(\mathbf{x}_b|\mathbf{x})) + const. \quad (2.6)$$

The analysis is now the value of \mathbf{x} that minimizes the cost function. In the context of variational DA, \mathbf{x} is usually referred to as the control vector. As noted by Fisher (2010),

the probability density functions of the background and observations can, for the case of Gaussian error distributions, be modeled as:

$$p(\mathbf{x}_b|\mathbf{x}) = b \exp\left[\frac{1}{2}(\mathbf{x} - \mathbf{x}_b)^T \mathbf{B}^{-1}(\mathbf{x} - \mathbf{x}_b)\right],$$

$$p(\mathbf{y}|\mathbf{x}) = o \exp\left[\frac{1}{2}(\mathbf{y} - H(\mathbf{x}))^T \mathbf{R}^{-1}(\mathbf{y} - H(\mathbf{x}))\right],$$

where b and o are normalization factors (Bouttier and Courtier, 1999). Thus, by choosing an appropriate value for the constant in Eq. (2.6), we arrive at the cost function for three dimensional variational DA, 3D-Var:

$$J(\mathbf{x}) = \frac{1}{2}(\mathbf{x} - \mathbf{x}_b)^T \mathbf{B}^{-1}(\mathbf{x} - \mathbf{x}_b) + \frac{1}{2}(\mathbf{y} - H(\mathbf{x}))^T \mathbf{R}^{-1}(\mathbf{y} - H(\mathbf{x})). \quad (2.7)$$

The notation 3D is used to emphasize the fact that the observation operator only contains spatial mapping between model and observations. It is common practice to use observations taken during a period of time, referred to as an assimilation window, and evaluate them as if they were valid at the same time. An expansion of H to include temporal mapping essentially yields the cost function of 4D-Var. However, as information is propagated in time according to physical laws, this must be reflected in the observation operator. It is convenient to group observations taken at the same time k and evaluate the cost function in the following form:

$$J(\mathbf{x}) = \frac{1}{2}(\mathbf{x} - \mathbf{x}_b)^T \mathbf{B}^{-1}(\mathbf{x} - \mathbf{x}_b) + \frac{1}{2} \sum_{k=0}^K (\mathbf{y}_k - G_k(\mathbf{x}_k))^T \mathbf{R}_k (\mathbf{y}_k - G_k(\mathbf{x}_k)). \quad (2.8)$$

The new observation operator G_k now includes an integration of a the numerical model from $t = 0$ to the time of evaluation, k , and takes the form $G_k = H_k M_{0 \rightarrow k}$, where M is the numerical model. This term also appears in its transposed form in Eq. (2.8), implying that the model must be run backwards, i.e. from the end of the assimilation window and back to its beginning. For a full numerical model, with many highly non-linear processes, this is virtually impossible. If we assume that M can be approximated by a linearization around the solution of the full non-linear model state over the course of the assimilation window by providing a tangent linear model (TLM), the problem is possible to solve. The transpose of the TLM, the so-called adjoint model (ADJ) can be derived, making integration backwards in time possible.

As a consequence of the assumption that H does not introduce any errors, the formulation of 4D-Var discussed so far assumes a perfect forecast model: given perfect initial conditions and forcing, the model will produce a perfect forecast. This formulation is called strong constraint 4D-Var. In reality though, errors do arise from imperfect model physics, parametrization of subgrid processes, numerical schemes etc. The assumption of a perfect model may be relaxed to yield weak constraint 4D-Var, with the addition of an extra term in the cost function, containing information on the model error and its covariance matrix. Describing the latter is, however, a non-trivial task.

To sum up the above, the following assumptions are made for strong constraint 4D-Var:

- The mean errors of both observations and the background are zero.
- There is no correlation between the observation errors and the background errors.
- The observation errors are uncorrelated in space and time.
- The errors are normally distributed (Gaussian).
- The forecast model is perfect — no error introduced by the observation operator.
- The evolution of the model over the assimilation window is approximately linear.
- The background is close to the true state.

4D-Var has the distinct advantage of evaluating the observations at their correct time, and through integration of both the TLM and the ADJ, the information is propagated backward and forward in time in accordance with the (linearized) model physics, allowing for an observation to affect the state upstream from its location as well as downstream. The drawback is the fact that it is necessary to maintain three separate model codes; the non-linear (NLM), the TLM and the ADJ. 4D-Var is also computationally demanding, particularly the ADJ. The tangent linear assumption poses a limit on the assimilation window length, as non-linearities will dominate the solution of the ocean model on longer time scales. This issue is particularly important for high-resolution models, as non-linear processes are better resolved. Weak constraint DA has the potential to compensate for the breach of the tangent linear assumption, allowing for longer windows.

Section 3.2 will cover how 4D-Var is implemented in ROMS, and how the cost function is minimized.

2.3 Observations

Observations are an essential component of an ocean assimilation system, but also provide invaluable information for validating non-assimilative models such as hindcasts and for determining the skill of an ocean forecast system. In general, observations are divided into two main categories based on how the measurements are obtained: in-situ or by the means of remote sensing.

For the case of the ocean, observations obtained through remote sensing are limited to the surface. In this thesis we have used two different types of remotely sensed observations: satellite sea surface temperature (SST) and HF radar surface currents. As the latter is the focus of paper I and II, and serves as a part of the observational network in paper IV, a detailed description of HF radars is given later in this section.

A common way to distinguish different SST products is by the level of processing the raw data has undergone to produce the end product. The instruments mounted on the satellites do not directly measure the surface temperature, and some sensors are unable to see through clouds. In order to provide an estimate of the SST with neither temporal nor spatial gaps it is thus necessary to combine observations from different sensors at different times. This can be done by applying optimal interpolation techniques (e.g. Donlon et al., 2012), and SST products derived this way are called level 4 (L4) products. However, this processing method causes some details (e.g. fronts) visible in the raw observations to be lost or smoothed out. In order to provide data

everywhere, the resolution in such products must also be coarser than that of lower level products. These constraints should be reflected in the error of representativeness provided to the assimilation system. In paper III two different L4 products of different horizontal resolutions and geographical coverage were used for assimilation, while in paper IV we used a level 2 (L2) product for the same purpose. The L2 product consists of SST observations from individual satellite passes projected onto a grid with 1.5 km resolution. As the observations are derived from infrared sensors, data are only available during cloud free conditions. When using this data set we take advantage of 4D-Var's capability to propagate information in time according to the linearized model physics. This could be beneficial for the multivariate response of the DA system, as the movement of fronts and eddies can be inferred from subsequent satellite passages. On the other hand, SST data are only available during cloud free conditions, which could cause a "fair weather" bias of the modeled temperature.

In addition to HF radar currents and SST, in-situ observations of temperature and salinity have also been used for assimilation. In-situ observations provide the only source of information of the sub-surface ocean, and contrary to observations obtained by remote sensing, the number of such observations are limited. The majority of the in-situ temperature and salinity observations used in this thesis are obtained by profiling CTDs during research cruises, but observations from a wide range of platforms such as Argo profiling floats, moorings, gliders, FerryBoxes, and along-track thermosalinograph measurements from vessels are also included in the data sets used for assimilation.

In paper I and paper II, in-situ measurements of ocean currents obtained by two different means are used for comparison with HF radar currents and as means for validation of the ocean model. A mooring with two acoustic Doppler current profilers (ADCP) provided a time series of the Eulerian vertical current profile for a location within the area covered by the HF radars. Two types of surface drifters, iSphere drifters, which are half-submerged, and self locating datum marker buoys (SLMDB), with a cross-shaped sail with average depth 0.7 m below the surface, were used to provide observations of the Lagrangian surface currents.

HF radars measure ocean currents based on the backscatter from surface waves (Stewart and Joy, 1974). The operating frequencies of HF radars lies within the range of 3-50MHz, which is close to the frequency bands of AM and FM radio (Paduan and Washburn, 2013). Depending on the operating frequency, HF radars can measure currents up to 200 km offshore, and they can operate under all weather conditions. As such, they provide an excellent platform for observing ocean surface currents over extensive areas in coastal regions.

The basic operation principle of a HF radar is to transmit an electromagnetic wave of wavelength λ , and receive the signal that is backscattered from the ocean surface. Backscattering occurs from waves of wavelength $\lambda/2$ that are traveling in a radial direction to or from the antenna. This is known as Bragg scattering, and will result in two distinct peaks in the frequency spectrum of the received signal, one caused by waves moving away from the antenna and one by waves moving towards it. In the absence of an underlying ocean current, and under the assumption of deep water waves, the peaks will be at frequencies corresponding to a Doppler shift due to the phase speed of the surface waves that reflected the signal, more specifically at $f_b = \pm g/\pi\lambda$. However, in the presence of an ocean current there will be an additional shift in frequency, Δf . The

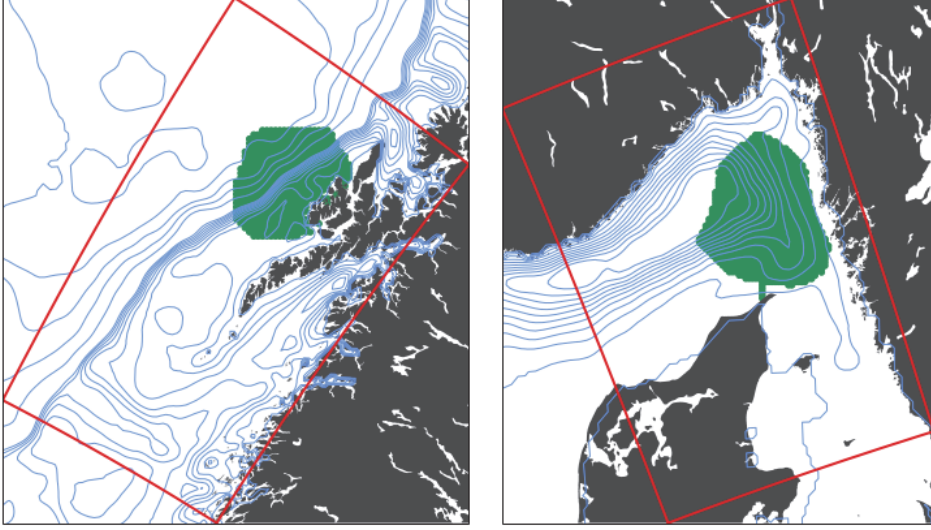


Figure 2.2: The coverage of the HF radar networks used in paper II (left) and paper IV (right). The model domains are shown in red, while the contours indicate the bathymetry.

radial velocity component (v_r) of the ocean current can thus be found by subtracting the theoretical phase speed (c_p) from the phase speed derived from the observed signal (c_p^{obs})

$$v_r = c_p^{obs} - c_p. \quad (2.9)$$

When the same patch of the ocean is simultaneously observed by two or more HF radars, their respective measured radial current components may be combined to form an estimate of the total current, i.e. the components in northerly and easterly directions (Gurgel, 1994). The level of precision of the current estimate will depend on the angle between the respective radials, with higher uncertainties as the angles become more and more parallel through geometric dilution of precision (Chapman et al., 1998).

While radial currents may be used directly for data assimilation through the specification of an observation operator, maps of total currents from a network of HF radars can provide information for monitoring ocean currents in real-time.

In this thesis observations from two HF radar networks, one in Vesterålen and one on the western coast of Sweden, are used. The operating frequencies were 13.525 MHz and 13.5 MHz, respectively. Fig. 2.2 shows the areas covered by the HF radar networks. Paper I uses radial currents from one of the antennas in Vesterålen, while the total currents provided by this network are assimilated in paper II. In paper IV the total currents from the Swedish HF radar network are assimilated.

Chapter 3

Tools and Methods

3.1 ROMS

The model experiments are performed with the Regional Ocean Modeling System (ROMS). The development of ROMS is led by groups at Rutgers University and University of California, Los Angeles (UCLA), with contributions from users around the world. ROMS is a hydrostatic, primitive equation ocean model, which uses split-explicit time stepping to solve the momentum equations (Shchepetkin and McWilliams, 2005, 2009). ROMS applies the Boussinesq approximation, meaning that density differences only affect vertical accelerations through the buoyancy term. It applies terrain-following vertical coordinates, which allows for higher resolution at depths of particular interest, such as the mixed layer. This coordinate system falls within the sigma type vertical coordinate, for which pressure gradient errors may be a problem, particularly in the presence of steep topography. Numerical algorithms to reduce this issue have been implemented in ROMS (Shchepetkin and McWilliams, 2003).

3.2 ROMS-4DVAR

A 4D-Var assimilation system has been developed for ROMS, mainly through efforts by a group at University of California, Santa Cruz. This section aims to give a brief overview of the methods applied in the scientific papers; a more thorough description of the DA system and its performance is given in Moore et al. (2011a,b,c).

The control vector in ROMS-4DVAR consists of the prognostic variables (surface elevation, barotropic and baroclinic velocities, temperature, and salinity) at the start of the assimilation window (t_0), with the possibility of expansion to include the surface forcing and lateral boundary conditions.

ROMS comes with three different implementations of 4D-Var. In this thesis we have used two: the incremental strong constraint 4D-Var (IS4DVAR) and the 4D physical space statistical analysis system (4DPSAS). To keep notation simple and in accordance with that of Sec. 2.2, the expansion of the control vector by surface forcing and boundary conditions will not be considered here.

The algorithms are based on departures from the background state, meaning that the state vector consists of the sum of two terms: the background state ($\mathbf{x}_b(t_0)$) and an increment ($\delta\mathbf{x}(t_0)$) that is assumed to be small compared with the background. This

is in accordance with the assumption that the background state is close to the true state. In both IS4DVAR and 4DPSAS, an iterative approach is used to find the solution that minimizes the cost function. During these iterations, the so-called inner-loops (denoted by subscript m in the following), the TLM and ADJ are used to propagate information forward and backward in time. To speed up convergence it is possible to update the non-linear solution according to an intermediate analysis increment and repeat the inner-loops with a linearization around the updated model state. Such re-linearizations are termed outer-loops, and denoted by the superscript k in the following. The use of an outer-loop can to a certain degree compensate for non-linearities within the assimilation window. The number of outer- and inner-loops to be used during the minimizations of the cost function are, in ROMS-4DVAR, most commonly specified by the user a priori.

IS4DVAR

Incremental, strong constraint 4D-Var follows the approach suggested by Courtier et al. (1994). The cost function is minimized using the following approach:

1. An integration of NLM over the assimilation window, using $\mathbf{x}_b(t_0)$ as initial conditions. During this integration the innovations between the observations and the background, $\mathbf{d} = \mathbf{y} - H(\mathbf{x}_b)$, are calculated. The inner-loops iterations are started with $\delta\mathbf{x}_1^k = 0$.
 - a) An integration of TLM to compute the cost function $J(\delta\mathbf{x})$ and the increments $\mathbf{H}\delta\mathbf{x}_m^k$.
 - b) An integration of ADJ to compute $\nabla J(\delta\mathbf{x})$.
 - c) Minimization using a conjugate gradient approach.
 - d) Update the analysis increment $\delta\mathbf{x}_m^k$.
2. An integration of NLM with updated initial conditions $\mathbf{x}(t_0) = \mathbf{x}_b(t_0) + \delta\mathbf{x}_m^k(t_0)$

Here, steps a–d are the inner-loops that are repeated several times, ideally until the solution has converged. When all inner-loops have been completed and step 2 has been executed, the inner-loops are repeated if the number of outer-loops is set to be more than one. In contrast to the more common approach of updating both innovations and the linearization model during outer loops, ROMS-4DVAR follows the approach of Bennett (2005), keeping the values obtained for the innovations (\mathbf{d}) during the first outer-loop for all later outer-loops (Moore et al., 2011c). The last iteration of step 2 yields the final analysis $\mathbf{x}_b + \delta\mathbf{x}_M^k$.

In IS4DVAR the value of the cost function decreases monotonically with the number of inner-loops. Solutions that minimize the cost function are sought after in the space spanned by the control vector, and thus always correspond to a physical solution. This means that even if the number of iterations is insufficient to ensure convergence of the solution, the result will be meaningful and closer to the true state than the first guess.

4DPSAS

The increments to the analysis, for simplicity named $\delta \mathbf{x}_a$, can according to Eqs. (2.1)-(2.3) be expressed as

$$\delta \mathbf{x}_a = \mathbf{x}_a - \mathbf{x}_b = \mathbf{B}\mathbf{H}^T(\mathbf{H}\mathbf{B}\mathbf{H}^T + \mathbf{R})^{-1}\mathbf{d}. \quad (3.1)$$

It can be further simplified by defining $\mathbf{w}_a = (\mathbf{H}\mathbf{B}\mathbf{H}^T + \mathbf{R})^{-1}\mathbf{d}$, whose dimension is the number of observations, and Eq. (3.1) is referred to as the dual formulation for 4D-Var, while 4D-Var in the form of the previously discussed IS4DVAR is called the primal formulation. For the case of an ocean DA system, the number of observations is typically much smaller than the number of entries in the state vector, thus searching for a solution in observation space rather than in model space may be advantageous. A new cost function can be defined as:

$$I(\mathbf{w}) = \frac{1}{2}\mathbf{w}^T(\mathbf{H}\mathbf{B}\mathbf{H}^T + \mathbf{R})\mathbf{w} - \mathbf{w}^T\mathbf{d}. \quad (3.2)$$

This is the cost function of 4DPSAS. Contrary to the primal formulation of 4D-Var, the dimension of the control vector in 4DPSAS remains the same when weak constraint is applied as the number of observations does not change. This formulation is thus much better suited when model errors are taken into account. The solution in 4DPSAS is found using the following iterative process:

1. An integration of NLM with initial conditions $\mathbf{x}(t_0) = \mathbf{x}_b(t_0)$, during which \mathbf{d} is calculated. Set $\mathbf{w}_1^k = \mathbf{d}$.
 - a) Integrate ADJ to compute $\mathbf{H}^T \mathbf{w}_m^k$.
 - b) Multiply by the covariance matrix to get $\mathbf{B}\mathbf{H}^T \mathbf{w}_m^k$.
 - c) Integrate TLM to compute $\mathbf{H}\mathbf{B}\mathbf{H}^T \mathbf{w}_m^k$.
 - d) Apply a conjugate gradient algorithm to get the cost function $I(\mathbf{w})$, which gives an estimate of \mathbf{w}_{m+1}^k .
2. Integrate ADJ to compute $\mathbf{H}^T \mathbf{w}_{m+1}^k$.
3. Multiply by the background covariance matrix to get $\mathbf{B}\mathbf{H}^T \mathbf{w}_{m+1}^k$.
4. An integration of NLM with updated initial conditions $\mathbf{x}(t_0) = \mathbf{x}_b(t_0) + \delta \mathbf{x}_k(t_0)$.

Similar to IS4DVAR, steps a–d are the steps performed in the inner-loops, while steps 1–4 are performed in the outer-loops. The final analysis is given by the last iteration of step 4.

Chapter 4

Summary and future perspective

In this PhD thesis we have investigated how the use of a 4D-Var ocean assimilation system impacts the circulation in high-resolution coastal models.

- **Paper I:** Investigates whether HF radar observations of currents include Stokes drift and what depth they represent. This is important to determine the suitability of this observing system for use in DA.
- **Paper II:** Evaluates the ability of the 4D-Var ocean assimilation system to realistically reproduce energetic slope currents by assimilating HF radar currents and CTD hydrography.
- **Paper III:** Examines how assimilation of hydrography affect the upper ocean circulation estimates, and the potential consequences for particle transport.
- **Paper IV:** Combining the experience from paper I-III, a reanalysis of the Kattegat-Skagerrak is produced and used to investigate the mechanisms causing variability in the onset of the Norwegian Coastal Current.

4.1 Summary of papers

Paper I: Comparison of HF radar measurements with Eulerian and Lagrangian surface currents

Röhrs, J., A. K. Sperrevik, K. H. Christensen, G. Broström, and Ø. Breivik

The aim of this study was to determine whether HF radar observations of currents include the Stokes drift, which is a mean drift velocity in the waves, and to identify which depth the observed currents correspond to. In order to use HF radar currents for data assimilation it is essential to know what the observations actually represent. To achieve this goal an observational campaign measuring surface currents by three different means was conducted: a HF radar antenna, an ADCP sampling vertical profiles of the Eulerian current, and two types of surface drifters sampling the Lagrangian current field. In addition, wave data were provided by a pressure sensor on the ADCP rig. According to the results of Röhrs et al. (2012) this observational system allows us to distinguish between Eulerian and Lagrangian currents. Our results showed good agreement between HF radar and Eulerian ADCP currents, and the best agreement with

currents from surface drifters was obtained when the Stokes drift, derived from wave data, were subtracted from the drifter velocities. Furthermore, our results showed that the HF radar currents represent a vertical average of currents, weighted by an exponential function with an e -folding scale in the range between 0.8 and 1.4 m, meaning that 80% of the signal comes from the upper meter. This is in accordance with the theoretical calculations by Stewart and Joy (1974).

Paper II: Constraining energetic slope currents through assimilation of high-frequency radar observations

Sperrevik, A. K., K. H. Christensen, and J. Röhrs

In this paper the impact of assimilation of HF radar total currents in a high-resolution model is investigated in order to determine the potential effect of such observations on the subsequent circulation estimates. The ability of the assimilation system to reproduce an energetic, non-linear slope current is first investigated by assimilating synthetic current observations in an idealistic model configuration mimicking the complex topography of the Lofoten/Vesterålen shelf, using different configurations of the assimilation system. Secondly, a series of assimilation experiments using a realistic model setup were performed:

- Assimilating only HF radar currents.
- Assimilating only CTD hydrography.
- Assimilating both HF radar currents and CTD hydrography.

For comparison, a model simulation without assimilation was also produced. Based on each updated initial state, forecast simulations of 5 days were conducted, and the results of these were compared with complementary observations from the SLMDB surface drifters and the ADCP mooring. The results showed positive impact of assimilation of HF radars on the forecast skill of upper ocean transport, with further improvement obtained when CTD hydrography was included. The CTD observations alone did, however, not provide sufficient information to constrain the circulation. This underlines the value of assimilating complementary observation sources.

Paper III: Impact of data assimilation on Eulerian versus Lagrangian estimates of upper ocean transport

Sperrevik, A. K., J. Röhrs, and K. H. Christensen

A common application of regional hindcasts is transport studies of biological quantities such as fish eggs and larvae. The coastal dynamics are, however, often not properly resolved in such hindcasts. This may result in erroneous description of the transport. As demonstrated by Myksvoll et al. (2014), vertical stratification impacts transport of cod eggs of different densities, highlighting the importance of realistic stratification in the model archives used for these purposes.

In this study a reanalysis for the first six months of 1984 was produced by assimilating SST and in-situ hydrography observations using the same model application as in paper II. This period was chosen as the Institute of Marine Research (IMR) conducted extensive field campaigns during the spring of 1984 to assess the stock of Northeast

Arctic cod, which have their main spawning grounds inside Vestfjorden, providing a unique data set of in-situ profiles. The changes in upper ocean circulation caused by improved representation of the water mass distribution, both in the vertical and the horizontal, are investigated by evaluating the impact on the Eulerian and Lagrangian surface currents. The results show similar distribution of the Eulerian current speeds compared with a traditional hindcast generated with the same model configuration, while the Lagrangian current speeds have overall higher kinetic energy in the reanalysis. One possible explanation for these differences is that the increased effective model resolution caused by stronger stratification allows for more small-scale circulation features to be generated.

Paper IV: On the variability in the onset of the Norwegian Coastal Current

Christensen, K. H., A. K. Sperrevik, and G. Broström

The most prominent feature of the coastal circulation along the coast of Norway is the Norwegian Coastal Current (NCC). It originates in the Skagerrak as a continuation of the outflow from the Baltic Sea, and flows northwards along the coast. Thus, it has profound impact on the environmental conditions all along the Norwegian coast, and a good description of this current is therefore of uttermost importance for coastal models in Norway.

In this study we generate a reanalysis of the circulation in Kattegat-Skagerrak with a horizontal resolution of 1 km, covering the period October 2014 - November 2015. The observational data set used consist of in-situ observations from multiple sources, high-resolution SST, and surface currents provided by two HF radar antennas on the Swedish coast. The reanalysis is used to investigate the variations in the onset of the NCC with emphasis on the response to large-scale wind forcing, and to evaluate how well the circulation correspond with conceptual models described in the literature. Our results reveal that the local wind forcing explains 75% of the variability of the transport in NCC.

The impact of different observation types on the transport in the NCC is evaluated using adjoint techniques as described in Moore et al. (2011b); Neveu et al. (2016). The results show similar impact of SST and HF radar currents observations, even though the HF observations are too far away from the section to directly observe the transport. Normalizing the impacts by the number of observations in each category reveals, however, that in-situ data by far have the largest impact per individual observation.

4.2 Perspectives

Adjusting the model state by the means of data assimilation can significantly improve model skill, both directly as well as implicitly. The result of paper III is an example of the latter: the first baroclinic Rossby radius is increased as a consequence of improved stratification achieved through assimilating in-situ profiles of temperature and salinity. As this scale is linked to the scale of boundary currents, fronts and eddies, an increase of the first baroclinic Rossby radius implies an increase in the scale of such circulation features as well. Thus, the model's ability to generate such features is affected.

The oceanic observational network is insufficient to properly constrain the circulation, especially for the case of high-resolution coastal models. This advocates for the use of advanced DA techniques such as the 4D-Var methods applied in the papers in this thesis (Talagrand, 1997), as the integrations of the linearized models backward and forward in time allows an observation to influence the ocean state both upstream and downstream of its actual location, and the (linearized) model physics ensure a multivariate response to each available observation.

The positive effect of complementing observations of the near-surface flow field with CTD profiles, as discussed in paper II, and the observation impact calculations performed in paper IV, which show contributions from all assimilated observation types on increments to the transport of the NCC, are in agreement with Oke et al. (2015a), who conclude that there are currently no redundant observation sources in ocean DA. These results provide motivation for a continued effort to include data from both existing and emerging observational platforms in future studies and operational forecast models. An important information source we have not taken advantage of in this thesis is sea surface height from satellite altimeters, which could provide valuable information on the large scale circulation patterns and complement HF radar currents. However, satellite altimetry products suffer from high uncertainties in the near-coastal zone (Cipollini et al., 2010), and particular care is required when including such data in high-resolution coastal models. One promising prospect in this regard is the planned SWOT mission (see <https://swot.jpl.nasa.gov/mission/>), which aims to provide high-resolution measurements of the sea surface height. Furthermore, the transition from assimilating HF radar total currents to direct assimilation of the radial current velocities is compelling for several reasons. Firstly, processing of the radials to total vectors introduce additional uncertainties to the observations. Secondly, the use of radials will expand the area where current observations are available. Direct assimilation of radials is also less vulnerable to failures in the infrastructure, as one antenna alone provide information that can be used by the assimilation system.

The encouraging results of the studies included in this thesis aside, there are still many aspects of the ocean DA system that can be improved and several challenges to be overcome, some general and some specific to the case of an operational DA forecast application. The performance of the DA system is sensitive to the specification of observational errors and the background error covariance matrix, both which are assumed to be known a priori. In our studies we have used an estimate of \mathbf{B} based on climatology calculated from multi-year simulations of the nonlinear model, a common approach in variational DA. This approach does not take the so-called errors of the day into account, and several studies have shown improvement of the analysis when static background errors covariances are combined with flow-dependent error covariances obtained from ensemble simulations to form \mathbf{B} (e.g. Bannister, 2017; Buehner, 2005; Gustafsson and Bojarova, 2014). The observational errors are also assumed known and explicitly specified to the system, and improvements to this component can certainly be made. Desroziers et al. (2005); Neveu et al. (2016) provide a method that can be used to improve the specification of \mathbf{R} .

The 4D-Var DA scheme used in this thesis are computationally costly, it is approximately 20-30 times as expensive to run as a stand-alone forecast model. This poses a challenge, especially for operational DA, and compromises to the design of the system in terms of assimilation window length and the number of iterations used to obtain

the minimum value of the cost function might be necessary. A common approach in many NWP centers is to perform the inner-loops at lower resolution than the non-linear model. The implementation of this approach in ROMS-4DVAR, holds the potential to reduce the computational cost significantly. Another challenge to operational DA is the delay with which many in-situ observations are made available. Considering the sparse number of such observations available for coastal circulation models, one might consider taking advantage of the long memory of the ocean and use seasonal reanalyses to re-initialize the operational DA system. Such seasonal reanalyses can also provide useful data sets for e.g. biological applications, which are often focused on evaluating a season in retrospect to investigate the conditions for e.g. recruitments to fish stocks and primary production.

References

- Ådlandsvik, B. and S. Sundby, 1994: Modelling the transport of cod larvae from the Lofoten area. *ICES Marine Science Symposia*, Vol. 198, 379–392. 1.1
- Bannister, R. N., 2017: A review of operational methods of variational and ensemble-variational data assimilation. *Q. J. R. Meteorol. Soc.*, **143** (703), 607–633, doi:10.1002/qj.2982. 4.2
- Bennett, A. F., 2005: *Inverse Modeling of the Ocean and Atmosphere*. Cambridge University Press. 3.2
- Bergthorsson, P. and B. R. Döös, 1955: Numerical Weather Map Analysis. *Tellus*, **7** (3), 329–340, doi:10.3402/tellusa.v7i3.8902. 2.2
- Blayo, E., M. Bocquet, E. Cosme, and L. F. Cugliandolo, 2014: *Advanced Data Assimilation for Geosciences*. 2.2
- Blockley, E. W., M. J. Martin, A. J. McLaren, A. G. Ryan, J. Waters, D. J. Lea, I. Mirouze, K. A. Peterson, A. Sellar, and D. Storkey, 2014: Recent development of the Met Office operational ocean forecasting system: an overview and assessment of the new Global FOAM forecasts. *Geosci. Model Dev.*, **7** (6), 2613–2638, doi:10.5194/gmd-7-2613-2014. 1.1
- Bouttier, F. and P. Courtier, 1999: Data assimilation concepts and methods. ECMWF, Lecture Notes NWP Course. 2.2, 2.2
- Breivik, Ø. and A. A. Allen, 2008: An operational search and rescue model for the Norwegian Sea and the North Sea. *J. Mar. Syst.*, **69** (1–2), 99–113, doi:10.1016/j.jmarsys.2007.02.010. 1.1
- Broström, G., A. Carrasco, L. R. Hole, S. Dick, F. Janssen, J. Mattsson, and S. Berger, 2011: Usefulness of high resolution coastal models for operational oil spill forecast: the "Full City" accident. *Ocean Sci.*, **7** (6), 805–820, doi:10.5194/os-7-805-2011. 1.1
- Budgell, W. P., 2005: Numerical simulation of ice-ocean variability in the Barents Sea region. *Ocean Dyn.*, **55** (3–4), 370–387, doi:10.1007/s10236-005-0008-3. 2.1
- Buehner, M., 2005: Ensemble-derived stationary and flow-dependent background-error covariances: Evaluation in a quasi-operational NWP setting. *Q.J.R. Meteorol. Soc.*, **131** (607), 1013–1043, doi:10.1256/qj.04.15. 4.2
- Chapman, R. D., L. K. Shay, and H. C. Graber, 1998: On the accuracy of HF radar surface current measurements: intercomparisons with ship-based sensors. *Oceanographic Lit. Rev.*, **3** (45), 578. 2.3
- Cipollini, P., J. Benveniste, J. Bouffard, W. Emery, C. Gommenginger, D. Griffin, J. Høyer, K. Madsen, F. Mercier, L. Miller, et al., 2010: The Role of Altimetry in Coastal Observing Systems. European Space Agency, 166–176, doi:10.5270/OceanObs09.cwp.16. 4.2

- Courtier, P., J.-N. Thépaut, and A. Hollingsworth, 1994: A strategy for operational implementation of 4d-Var, using an incremental approach. *Q. J. R. Meteorol. Soc.*, **120** (519), 1367–1387, doi:10.1002/qj.49712051912. 3.2
- Desroziers, G., L. Berre, B. Chapnik, and P. Poli, 2005: Diagnosis of observation, background and analysis-error statistics in observation space. *Q. J. R. Meteorol. Soc.*, **131** (613), 3385–3396, doi:10.1256/qj.05.108. 4.2
- Donlon, C. J., M. Martin, J. Stark, J. Roberts-Jones, E. Fiedler, and W. Wimmer, 2012: The Operational Sea Surface Temperature and Sea Ice Analysis (OSTIA) system. *Remote Sens. Environ.*, **116**, 140–158, doi:10.1016/j.rse.2010.10.017. 2.3
- Fisher, M., 2010: Data assimilation lecture notes. ECMWF, Lecture Notes NWP Course. 2.2, 2.2
- Gundlach, E. R. and M. O. Hayes, 1978: Vulnerability of coastal environments to oil spill impacts. *Mar. Technol. Soc. Rev.*, **12** (4). 1.1
- Gurgel, K. W., 1994: Shipborne measurement of surface current fields by HF radar. *OCEANS '94. 'Oceans Engineering for Today's Technology and Tomorrow's Preservation.'* Proceedings, Vol. 3, III/23–III/27 vol.3, doi:10.1109/OCEANS.1994.364167. 2.3
- Gustafsson, N. and J. Bojarova, 2014: Four-dimensional ensemble variational (4d-En-Var) data assimilation for the HIgh Resolution Limited Area Model (HIRLAM). *Nonlin. Processes Geophys.*, **21** (4), 745–762, doi:10.5194/npg-21-745-2014. 4.2
- Hannah, C. G., C. E. Naimie, J. W. Loder, and F. E. Werner, 1997: Upper-ocean transport mechanisms from the Gulf of Maine to Georges Bank, with implications for Calanus supply. *Cont. Shelf Res.*, **17** (15), 1887–1911, doi:10.1016/S0278-4343(97)00048-4. 1.1
- Ihaksi, T., T. Kokkonen, I. Helle, A. Jolma, T. Lecklin, and S. Kuikka, 2011: Combining Conservation Value, Vulnerability, and Effectiveness of Mitigation Actions in Spatial Conservation Decisions: An Application to Coastal Oil Spill Combating. *J. Environ. Manage.*, **47** (5), 802–813, doi:10.1007/s00267-011-9639-y. 1.1
- Isachsen, P. E., I. Koszalka, and J. H. LaCasce, 2012: Observed and modeled surface eddy heat fluxes in the eastern Nordic Seas. *J. Geophys. Res.: Oceans*, **117** (C8), C08 020, doi:10.1029/2012JC007935. 2.1
- Jordi, A., M. I. Ferrer, G. Vizoso, A. Orfila, G. Basterretxea, B. Casas, A. Álvarez, D. Roig, B. Garau, M. Martínez, V. Fernández, A. Fornés, M. Ruiz, J. J. Fornós, P. Balaguer, C. M. Duarte, I. Rodríguez, E. Alvarez, R. Onken, P. Orfila, and J. Tintoré, 2006: Scientific management of Mediterranean coastal zone: A hybrid ocean forecasting system for oil spill and search and rescue operations. *Mar. Pollut. Bull.*, **53** (5–7), 361–368, doi:10.1016/j.marpolbul.2005.10.008. 1.1
- Kalnay, E., 2003: *Atmospheric Modeling, Data Assimilation and Predictability*. Cambridge University Press. 2.2

- Lien, V. S., Y. Gusdal, J. Albretsen, A. Melsom, and F. B. Vikebø, 2013: Evaluation of a Nordic Seas 4 km numerical ocean model hindcast archive (SVIM), 1960-2011. *Fisken og Havet*, 7–79. 2.1
- Lorenz, E. N., 1963: Deterministic Nonperiodic Flow. *J. Atmos. Sci.*, **20** (2), 130–141, doi:10.1175/1520-0469(1963)020<0130:DNF>2.0.CO;2. 2.2
- Mitarai, S., D. A. Siegel, J. R. Watson, C. Dong, and J. C. McWilliams, 2009: Quantifying connectivity in the coastal ocean with application to the Southern California Bight. *J. Geophys. Res.: Oceans*, **114** (C10), C10026, doi:10.1029/2008JC005166. 1.1
- Moore, A. M., H. G. Arango, G. Broquet, C. Edwards, M. Veneziani, B. Powell, D. Foley, J. D. Doyle, D. Costa, and P. Robinson, 2011a: The Regional Ocean Modeling System (ROMS) 4-dimensional variational data assimilation systems: Part II – Performance and application to the California Current System. *Prog. Oceanogr.*, **91** (1), 50–73, doi:10.1016/j.pocean.2011.05.003. 3.2
- , 2011b: The Regional Ocean Modeling System (ROMS) 4-dimensional variational data assimilation systems: Part III – Observation impact and observation sensitivity in the California Current System. *Prog. Oceanogr.*, **91** (1), 74–94, doi:10.1016/j.pocean.2011.05.005. 3.2, 4.1
- Moore, A. M., H. G. Arango, G. Broquet, B. S. Powell, A. T. Weaver, and J. Zavala-Garay, 2011c: The Regional Ocean Modeling System (ROMS) 4-dimensional variational data assimilation systems: Part I – System overview and formulation. *Prog. Oceanogr.*, **91** (1), 34–49, doi:10.1016/j.pocean.2011.05.004. 3.2, 3.2
- Myksovoll, M. S., K.-M. Jung, J. Albretsen, and S. Sundby, 2014: Modelling dispersal of eggs and quantifying connectivity among Norwegian coastal cod subpopulations. *ICES J. Mar. Sci.*, **71** (4), 957–969, doi:10.1093/icesjms/fst022. 1.1, 4.1
- Neveu, E., A. M. Moore, C. A. Edwards, J. Fiechter, P. Drake, W. J. Crawford, M. G. Jacox, and E. Nuss, 2016: An historical analysis of the California Current circulation using ROMS 4d-Var: System configuration and diagnostics. *Ocean Modell.*, **99**, 133–151, doi:10.1016/j.ocemod.2015.11.012. 4.1, 4.2
- Oke, P. R., G. Larnicol, Y. Fujii, G. C. Smith, D. J. Lea, S. Guinehut, E. Remy, M. A. Balmaseda, T. Rykova, D. Surcel-Colan, M. J. Martin, A. A. Sellar, S. Mulet, and V. Turpin, 2015a: Assessing the impact of observations on ocean forecasts and reanalyses: Part 1, Global studies. *J. Oper. Oceanogr.*, **8**, s49–s62, doi:10.1080/1755876X.2015.1022067. 1.1, 4.2
- Oke, P. R., G. Larnicol, E. M. Jones, V. Kourafalou, A. K. Sperrevik, F. Carse, C. A. S. Tanajura, B. Mourre, M. Tonani, G. B. Brassington, M. L. Henaff, G. R. H. Jr, R. Atlas, A. M. Moore, C. A. Edwards, M. J. Martin, A. A. Sellar, A. Alvarez, P. D. Mey, and M. Iskandarani, 2015b: Assessing the impact of observations on ocean forecasts and reanalyses: Part 2, Regional applications. *J. Oper. Oceanogr.*, **8**, s63–s79, doi:10.1080/1755876X.2015.1022080. 1.1

- Paduan, J. D. and L. Washburn, 2013: High-frequency radar observations of ocean surface currents. *Annu. Rev. Mar. Sci.*, **5**, 115–136, doi:10.1146/annurev-marine-121211-172315. 2.3
- Röhrs, J. and K. H. Christensen, 2015: Drift in the uppermost part of the ocean. *Geophys. Res. Lett.*, **42** (23), 2015GL066733, doi:10.1002/2015GL066733. 1.1
- Röhrs, J., K. H. Christensen, L. R. Hole, G. Broström, M. Drivdal, and S. Sundby, 2012: Observation-based evaluation of surface wave effects on currents and trajectory forecasts. *Ocean Dyn.*, **62** (10–12), 1519–1533, doi:10.1007/s10236-012-0576-y. 4.1
- Røed, L. P. and J. Albrechtsen, 2007: The impact of freshwater discharges on the ocean circulation in the Skagerrak/northern North Sea area Part I: model validation. *Ocean Dyn.*, **57** (4–5), 269–285, doi:10.1007/s10236-007-0122-5. 2.1
- Saetre, R., (Ed.), 2007: *The Norwegian Coastal Current: Oceanography and Climate*. Fagbokforlaget, Trondheim. 2.1
- Sakov, P., F. Counillon, L. Bertino, K. A. Lisæter, P. R. Oke, and A. Korabely, 2012: TOPAZ4: an ocean-sea ice data assimilation system for the North Atlantic and Arctic. *Ocean Sci.*, **8** (4), 633–656, doi:10.5194/os-8-633-2012. 1.1
- Shchepetkin, A. F. and J. C. McWilliams, 2003: A method for computing horizontal pressure-gradient force in an oceanic model with a nonaligned vertical coordinate. *J. Geophys. Res.: Oceans*, **108** (C3), 3090, doi:10.1029/2001JC001047. 3.1
- , 2005: The regional oceanic modeling system (ROMS): a split-explicit, free-surface, topography-following-coordinate oceanic model. *Ocean Modell.*, **9** (4), 347–404, doi:10.1016/j.ocemod.2004.08.002. 3.1
- , 2009: Computational Kernel Algorithms for Fine-Scale, Multiprocess, Long-time Oceanic Simulations. *Handbook of Numerical Analysis*, Tribbia, R. M. T. a. J. J., Ed., Elsevier, Special Volume: Computational Methods for the Atmosphere and the Oceans, Vol. 14, 121–183, DOI: 10.1016/S1570-8659(08)01202-0. 3.1
- Stewart, R. H. and J. W. Joy, 1974: HF radio measurements of surface currents. *Deep Sea Res.*, **21** (12), 1039–1049, doi:10.1016/0011-7471(74)90066-7. 2.3, 4.1
- Svendsen, E., M. Skogen, P. Budgell, G. Huse, J. Erik Stiansen, B. Ådlandsvik, F. Vikebø, L. Asplin, and S. Sundby, 2007: An ecosystem modeling approach to predicting cod recruitment. *Deep Sea Res. Part II*, **54** (23–26), 2810–2821, doi:10.1016/j.dsr2.2007.07.033. 1.1
- Talagrand, O., 1997: Assimilation of Observations, an Introduction. *J. Meteorolog. Soc. Jpn.*, **75** (1B), 191–209. 2.2, 4.2
- Vikebø, F., C. Jørgensen, T. Kristiansen, and Ø. Fiksen, 2007: Drift, growth, and survival of larval Northeast Arctic cod with simple rules of behaviour. *Mar. Ecol. Prog. Ser.*, **347**, 207–219, doi:10.3354/meps06979. 1.1

Warner, T. T., R. A. Peterson, and R. E. Treadon, 1997: A Tutorial on Lateral Boundary Conditions as a Basic and Potentially Serious Limitation to Regional Numerical Weather Prediction. *Bull. Am. Meteorol. Soc.*, **78**, 2599–2617, doi:10.1175/1520-0477(1997)078<2599:ATOLBC>2.0.CO;2. 1.1

Winther, N. G. and G. Evensen, 2006: A hybrid coordinate ocean model for shelf sea simulation. *Ocean Modell.*, **13** (3–4), 221–237, doi:10.1016/j.ocemod.2006.01.004. 2.1